Computers and Concrete, *Vol. 14, No. 1 (2014) 59-71*
DOI: http://dx.doi.org/10.12989/cac.2014.14.1.059

New analytical model for the hoop contribution to the shear capacity of circular reinforced concrete columns

Francesco Trentadue[1], Giuseppe Quaranta[*2], Rita Greco[1] and Giuseppe Carlo Marano[1]

[1]Department of Civil Engineering and Architecture, Technical University of Bari, via E. Orabona 4, 70100 Bari, Italy
[2]Department of Structural and Geotechnical Engineering, Sapienza University of Rome, via Eudossiana 18, 00184 Rome, Italy

(*Received December 7, 2012, Revised April 14, 2014, Accepted May 18, 2014*)

Abstract. The paper is concerned with the analytical description of a resistance mechanism, not considered in previous models, by which the hoops contribute to the shear capacity of RC columns with circular cross sections. The difference from previous approaches consists in observing that, because of deformation, the hoops change their original shape and, as a consequence, their slope does not match anymore the original one in the neighborhood of a crack. The model involves two parameters only, namely the crack inclination and the hoop strain in the neighborhood of a crack. A closed-form analytical formulation to correlate the average value of the crack width and the hoop strain is also provided. Results obtained using the proposed model have been compared with experimental data, and a satisfactory agreement is found.

Keywords: circular column; cracked concrete; hoop; reinforced concrete; shear capacity

1. Introduction

The analysis of columns in reinforced concrete (RC) constructions subjected to lateral loads (e.g. wind pressure or earthquake ground motion) remains an area of concern for structural engineers (Sezen 2008). The shear capacity of such RC members can be calculated by considering the resistance mechanisms of concrete and transversal reinforcement. Typical concrete-based resistance mechanics are the shear stress transferred by compressed zones, the dowel action, the aggregates interlock and the so-called arch effect. These resistance mechanisms depend on many factors, such as the tensile longitudinal steel ratio, the concrete grade, the axial load level, and the aggregates size. The evaluation of this contribution is still a debated topic, and is essentially based on empirical or semi-empirical approaches. The second contribution to the shear capacity accounts for shear reinforcement-based resistance mechanisms, and it is usually formulated using a truss-based analogy. Among the others, circular RC columns can be preferred in place of rectangular-shaped members because of architectural reasons and the strength-invariance with respect to the loading direction. Although the state-of-the-practice for RC buildings and bridges makes extensive

*Corresponding author, Assistant Professor, E-mail: giuseppe.quaranta@uniroma1.it

http://www.techno-press.org/?journal=cac&subpage=8 ISSN: 1598-8198 (Print), 1598-818X (Online)

use of columns with circular cross sections, most of the current technical codes and guidelines usually provides specific design rules for RC columns with rectangular cross sections only. On the contrary, the shear capacity of a circular RC member is evaluated by means of some rules in which is implicitly assumed that the resistance is somewhat reducible to that of a member with an "equivalent" rectangular cross section. Following this approach, the shear strength model does not explicitly take into account the effects due to the shape of the cross section. So doing, it is not shown, therefore, to what extent the hoops contribute to the shear capacity, and how much this contribution differs from that of rectangular stirrups. One of the first model for the evaluation of the shear capacity of circular RC columns was presented by Ang *et al*. (1989). On addressing the shear strength of circular columns subjected to cyclic loading, these authors proposed a model in which the shear crack inclination was obtained on the basis of the lower bound plasticity, and a truss-based mechanism with fixed angle (equal to 45°) was introduced to evaluate the shear reinforcement capacity. This approach attracted considerable attentions, and motivated further researches (Wong *et al*. 1993, Priestly *et al*. 1994, Kowalsky and Priestley 2000). An attempt in exploring new resistance mechanisms for calculating the contribution of curved transverse reinforcement was done by Merta (2007). In that study, a deviatoric shear resistance mechanism of the hoops was identified and modeled as a concrete contribution to be added to the shear reinforcement capacity. This novel contribution was recognized by noting that a curved reinforcing bar under tension induces a compression state in radial direction which should be taken into account in order to define a shear resistance mechanism due to the hoops. Jensen and Hoang (2009) evaluated the shear strength of circular RC members by extending the plasticity-based crack sliding model originally developed for RC beams with rectangular cross section. In this work, the inclination of the crack was obtained by equating the load required to develop the crack to that needed to cause its sliding. A recent proposal was also presented by Turmo *et al*. (2009). These authors illustrated a formulation for evaluating the shear transferred by spiral reinforcement in solid members. Moreover, their work also considered the calculation of hollow core circular columns with both vertical and spiral reinforcement. In order to develop consistent theoretical models, the examination of experimental evidences about the behavior of circular RC columns is important. By analyzing several experimental data, Clarke and Birjandi (1993) concluded that the shear capacity of circular RC columns can be approximated using the approach for rectangular sections in (BS 5400, 1990), with some minor modifications. An artificial neural network based data-driven procedure was implemented by Caglar (2009) to determine the shear strength of circular reinforced concrete columns. More recently, Jensen *et al*. (2010) presented experimental results on heavily shear reinforced circular concrete members.

This paper introduces a new point-of-view for the analysis of the hoop contribution to the shear capacity of circular RC columns. The reinforcement shear capacity is here calculated by observing that, because of deformation, the hoops change their original shape in the neighborhood of a crack and, as a consequence, their slope does not match the original one. Starting from this consideration, an analytical model has been derived in order to estimate the contribution of the transversal reinforcement in circular RC columns. Therefore, the proposed model has the merit of describing analytically a mechanism, not yet investigated in previous models, by which the hoops contribute to the shear capacity of RC columns with circular cross sections. Numerical results obtained using the proposed model have been compared with experimental data, and a satisfactory agreement is found.

2. Shear capacity of circular reinforced concrete columns

2.1 Concrete shear capacity

The total shear capacity V of RC columns can be evaluated as follows:

$$V = V_c + V_s, \tag{1}$$

where V_c and V_s are the concrete and the reinforcement shear contribution, respectively. Although this paper is basically concerned with a new analytical model for V_s, the concrete shear capacity V_c must be considered because the comparison with experimental data will be performed on the basis of the predicted total shear capacity V in Eq. (1). In doing so, no *a priori* restrictions are imposed by the proposed reinforcement shear capacity model, and then V_c can be estimated by selecting one among the numerous models existing in the available literature. In this study, V_c [N] is obtained by means of the formulation proposed in (Merta 2007), that is:

$$V_c = \left(3.7\rho_l + 0.18 + 0.08\left(\frac{P}{A_g}\right)0.3 \right) k\sqrt{f_c'}\left(0.70A_g\right), \tag{2}$$

where ρ_l is the longitudinal reinforcement ratio, P/A_g is the average compressive stress (being P [N] the axial load and A_g [mm^2] the section gross area) and f_c' [N/mm^2] is the uniaxial cylinder compressive strength. Merta (2007) experimentally carried out the influence of the main variables on the concrete shear capacity model by analyzing a total of 44 data of circular cross section specimens without shear reinforcement under monotonic load. The term $0.70A_g$ represents the section's effective shear area. The shear enhancement coefficient k is

$$k = \begin{cases} 1.00 & a/D > 2.50 \\ 1.25 & a/D \le 2.50 \end{cases}, \tag{3}$$

where a is the shear-span and D is the section's diameter.

2.2 Proposed reinforcement shear capacity

A new reinforcement shear capacity model for circular RC columns is here described. To this end, a circular section crossed by a crack with constant width $\overline{BB'}$ is assumed, as shown in Fig. 1a (for sake of clarity, the crack width in the figures has been amplified and the longitudinal reinforcement is hidden). An arc AB' of the hoop in the neighborhood of the shear crack is considered, and it is subjected to a strain ε. It is assumed that – because of the tensile stress acting on it – this arc spalls the concrete cover and takes the rectilinear configuration AB. Before the crack opening, the length of the arc AB' is $2R\delta$ (with R and δ shown in Fig. 1a) whereas, once the crack is opened, its length $\overline{AB}$ becomes $2R\delta$ (1 + ε). Because of the symmetry, the two elements in which the circular section is divided by the crack are subjected to a relative vertical displacement. Hence, the following relation holds:

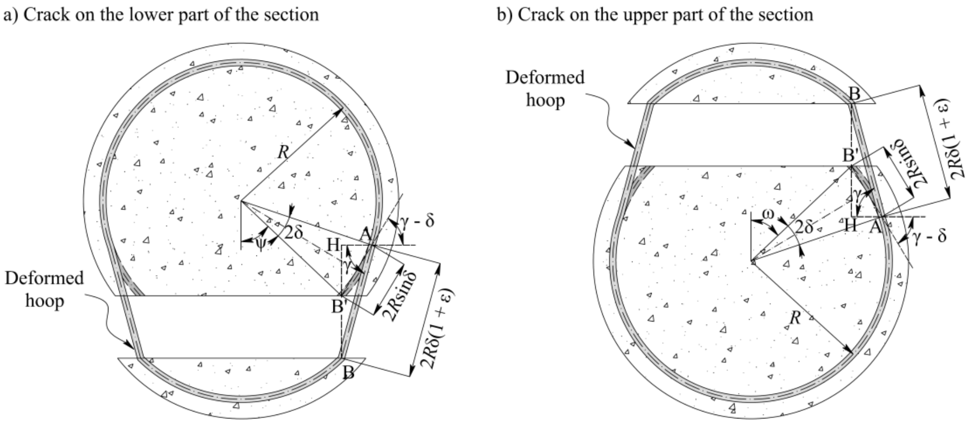

Fig. 1 Circular cross section crossed by crack

$$\overline{\mathrm{AH}} = 2R\delta(1+\varepsilon)\cos\gamma = 2R\sin\delta\cos(\gamma-\delta), \tag{4}$$

where γ is the angle shown in Fig. 1a. By introducing the angle $\psi = \gamma - 2\delta$, Eq. (4) yields:

$$(1+\varepsilon)\cos(\psi+2\delta) = \frac{\sin\delta}{\delta}\cos(\psi+\delta). \tag{5}$$

Eq. (5) holds for $\psi \le \pi/2$. If the crack takes place in the upper part of the section, then Eq. (5) is modified by replacing ψ with ω (see Fig. 1b).

Since the angle δ is small, the following series expansions can be considered when the crack occurs in the lower part of the circular section:

$$\cos(\psi+2\delta) = \cos\psi - 2\delta\sin\psi - 2\delta^2\cos\psi + o(\delta^2), \tag{6}$$

$$\cos(\psi+\delta) = \cos\psi - \delta\sin\psi - \frac{\delta^2}{2}\cos\psi + o(\delta^2), \tag{7}$$

$$\frac{\sin\delta}{\delta} = 1 - \frac{\delta^2}{6} + o(\delta^2). \tag{8}$$

By using Eqs. (6)-(8), Eq. (5) is rewritten as follows:

$$\begin{aligned}&(1+\varepsilon)\left(\cos\psi - 2\delta\sin\psi - 2\delta^2\cos\psi + o(\delta^2)\right) - \\ &\left(1 - \frac{\delta^2}{6} + o(\delta^2)\right)\left(\cos\psi - \delta\sin\psi - \frac{\delta^2}{2}\cos\psi + o(\delta^2)\right) = 0.\end{aligned} \tag{9}$$

After some manipulations, the following quadratic equation is obtained from Eq. (9):

$$\varepsilon - \delta(1+2\varepsilon)\tan\psi - \delta^2\left(\frac{4}{3} + 2\varepsilon\right) + o(\delta^2) = 0, \tag{10}$$

whose solution is:

$$\delta\left(\tan\psi,\varepsilon\right)=\frac{1}{\left(\frac{8}{3}+4\varepsilon\right)}\left(-\left(1+2\varepsilon\right)\tan\psi+\sqrt{8\varepsilon\left(\frac{2}{3}+\varepsilon\right)+\left(\left(1+2\varepsilon\right)\tan\psi\right)^{2}}\right). \tag{11}$$

If the crack occurs in the upper part of the section, then δ is evaluated by replacing ψ with ω in Eq. (11). Furthermore, for simplicity, the hoops are replaced with a smeared distribution of transversal reinforcement whose area per unit of length is A_{sh}/s, where A_{sh} is the area of the shear reinforcement and s is the spacing. It is assumed that a crack forms an angle θ with respect to the longitudinal axis of the column (see Fig. 2). This crack crosses the longitudinal section from the lower edge up to the neutral axis. The distance between the neutral axis and the upper edge of the section is d. With these premises, the following relations hold:

$$\begin{array}{ll}\cos\psi=\eta & \cos\omega=-\eta\\ \sin\psi=\sqrt{1-\eta^{2}} & \sin\omega=\sqrt{1-\eta^{2}}\\ \tan\psi=\sqrt{1-\eta^{2}}\Big/\eta & \tan\omega=-\sqrt{1-\eta^{2}}\Big/\eta\end{array}. \tag{12}$$

The reinforcement shear capacity of a ring with infinitesimal length equal to d$y$cotθ is now considered (see Fig. 2). This ring passes through the crack at the point B, which identifies the angle ψ. Let dV_s be the infinitesimal contribution of the ring. When the crack occurs in the lower part of the section, the contribution dV_s is:

$$\begin{aligned}\mathrm{d}V_s&=f_{yh}\left(\frac{A_{sh}}{s}\mathrm{d}y\cot\theta\right)\sin\gamma=f_{yh}\left(\frac{A_{sh}}{s}\mathrm{d}y\cot\theta\right)\sin\left(\psi+2\delta_{\psi}\right)\\&=f_{yh}R\frac{A_{sh}}{s}\cot\theta\left(\sin\psi\cos2\delta_{\psi}+\cos\psi\sin2\delta_{\psi}\right)\mathrm{d}\eta\\&=f_{yh}R\frac{A_{sh}}{s}\cot\theta\left(\sqrt{1-\eta^{2}}\cos2\delta_{\psi}+\eta\sin2\delta_{\psi}\right)\mathrm{d}\eta,\end{aligned} \tag{13}$$

where $\delta_{\psi}=\delta\left(\sqrt{1-\eta^{2}}\Big/\eta,\varepsilon\right)$ and f_{yh} is the yielding stress of the transversal reinforcement. If the crack takes place in the upper part of the section, then the infinitesimal contribution dV_s is

$$\begin{aligned}\mathrm{d}V_s&=f_{yh}\left(\frac{A_{sh}}{s}\mathrm{d}y\cot\theta\right)\sin\left(\omega+2\delta_{\omega}\right)=f_{yh}\left(\frac{A_{sh}}{s}\mathrm{d}y\cot\theta\right)\sin\left(\omega+2\delta_{\omega}\right)\\&=f_{yh}R\frac{A_{sh}}{s}\cot\theta\left(\sin\omega\cos2\delta_{\omega}+\cos\omega\sin2\delta_{\omega}\right)\mathrm{d}\eta\\&=f_{yh}R\frac{A_{sh}}{s}\cot\theta\left(\sqrt{1-\eta^{2}}\cos2\delta_{\omega}-\eta\sin2\delta_{\omega}\right)\mathrm{d}\eta,\end{aligned} \tag{14}$$

where $\delta_{\omega}=\delta\left(-\sqrt{1-\eta^{2}}\Big/\eta,\varepsilon\right)$. Finally, the reinforcement shear capacity is evaluated by integration, thus obtaining:

$$V_s = \Omega\left(d/R, \varepsilon\right) f_{yh} \frac{A_{sh}}{s} \left(2R\right) \cot\theta, \tag{15}$$

where $\Omega(d/R,\varepsilon)$ is the following integral:

$$\Omega\left(d/R, \varepsilon\right) = \frac{1}{2}\left(\begin{array}{l} \int_{-1+d/R}^{0}\left(\sqrt{1-\eta^2}\cos 2\delta_\omega - \eta\sin 2\delta_\omega\right)d\eta + \\ \int_{0}^{1}\left(\sqrt{1-\eta^2}\cos 2\delta_\psi + \eta\sin 2\delta_\psi\right)d\eta \end{array} \right). \tag{16}$$

The integral in Eq. (16) can be calculated numerically. In order to facilitate the use of Eq. (15), numerical values of Ω ($d/R,\varepsilon$) can be listed by evaluating the integral in Eq. (16) for some values of d/R and ε (see Table 1). As expected and as inferred from Table 1, the shear capacity attributable to the transversal reinforcement grows as the strain ε increases.

It is evident that the proposed formulation for V_s depends on two parameters (namely, θ and ε). As heuristic rule, the angle θ can be taken as 30°, thus resulting cot (30°) = 1.7321. This is a quite typical recommendation (Turmo *et al*. 2009, Priestley *et al*. 1996), and it is consistent with some building codes (for instance, the European code for RC structures imposes $1 \leq \cot\theta \leq 2.5$, and thus 1.7321 approximately falls in-between this range). Although refined theoretically-based models were recently proposed to calculate this angle (Jensen and Hoang 2009), $\theta = 30°$ is also assumed in this study. It is understood, however, that any other experimental-based rule or theoretical model

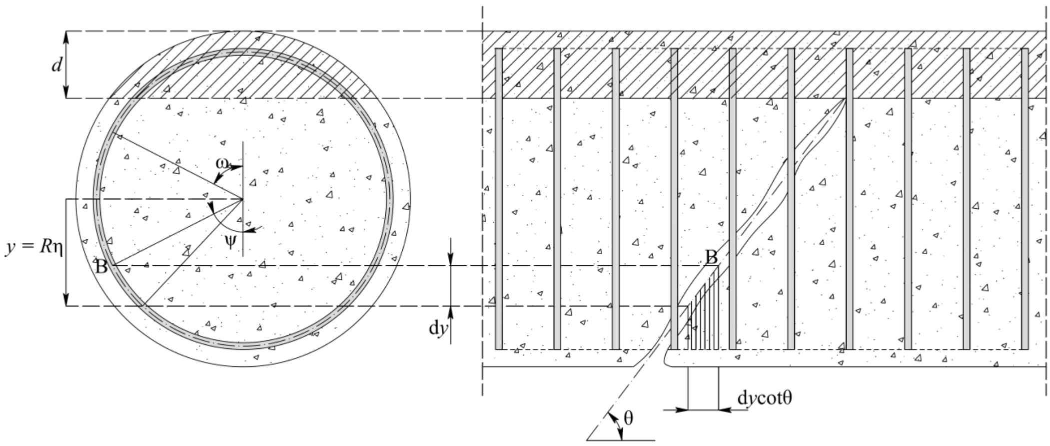

Fig. 2 A crack forming an angle θ with respect to the longitudinal axis of the column

Table 1 Numerical values for Ω ($d/R,\varepsilon$).

ε	$\Omega(d/R = 0.10,\varepsilon)$	$\Omega(d/R = 0.20,\varepsilon)$	$\Omega(d/R = 0.30,\varepsilon)$
0	0.771	0.744	0.711
1/100	0.781	0.753	0.719
5/100	0.809	0.778	0.741
10/100	0.834	0.799	0.762

Table 2 Experimental data (Clarke and Birjandi 1993) and numerical results

Specimen	D [mm]	D' [mm]	ρ_l [%]	P [kN]	a [mm]	f_c' [MPa]	f_{yh} [MPa]	A_{sh}/s [mm]	V_{exp} [kN]	V_{num} [kN]
M1/2	152	126	2.22	0.0	210	23.8	250	0.57	45	44
M1/3	152	126	2.22	0.0	230	23.8	250	0.57	46	44
M1/4	152	126	2.22	0.0	240	23.8	250	0.57	38	44
7a	300	252	2.3	0.0	230	29.2	250	0.67	262	145
11a	300	252	5.6	0.0	560	20.5	250	0.67	186	162
11b	300	252	5.6	0.0	560	20.5	250	0.67	188	162
12a	300	252	5.6	0.0	560	20.2	250	1.34	211	214
12b	300	252	5.6	0.0	560	20.2	250	1.34	239	214
13a	300	252	5.6	0.0	560	41.1	250	0.67	227	209
13b	300	252	5.6	0.0	560	41.1	250	0.67	228	209
14a	300	252	5.6	0.0	560	42.9	250	1.34	279	267
14b	300	252	5.6	0.0	560	42.9	250	1.34	288	267
15a	300	252	3.6	0.0	560	20.7	250	0.67	145	143
15b	300	252	3.6	0.0	560	20.7	250	0.67	148	143
16a	300	252	3.6	0.0	560	39.7	250	0.67	185	178
16b	300	252	3.6	0.0	560	39.7	250	0.67	186	178
17a	300	254	2.3	0.0	560	20.1	250	0.38	117	105
17b	300	254	2.3	0.0	560	20.1	250	0.38	115	105
19a	300	254	3.6	0.0	560	22.6	250	0.38	113	123
19b	300	254	3.6	0.0	560	22.6	250	0.38	129	123
20a	300	254	3.6	0.0	560	41.9	250	0.38	149	158
20b	300	254	3.6	0.0	560	41.9	250	0.38	137	158
21a	300	254	5.6	0.0	560	18.9	250	0.38	131	133
21b	300	254	5.6	0.0	560	18.9	250	0.38	151	133
22a	300	254	5.6	0.0	560	38.7	250	0.38	163	179
22b	300	254	5.6	0.0	560	38.7	250	0.38	164	179
23a	300	254	2.3	0.0	560	21.3	250	0.38	101	108
23b	300	254	2.3	0.0	560	21.3	250	0.38	113	108
24a	300	254	2.3	0.0	560	41.7	250	0.38	114	139
24b	300	254	2.3	0.0	560	41.7	250	0.38	128	139
25a	300	254	3.6	0.0	560	20.7	250	0.38	98	118
25b	300	254	3.6	0.0	560	20.7	250	0.38	122	118
26a	300	254	3.6	0.0	560	40.0	250	0.38	114	155
26b	300	254	3.6	0.0	560	40.0	250	0.38	150	155
27a	300	254	3.6	0.0	560	19.4	250	0.38	125	116
27b	300	254	5.6	0.0	560	19.4	250	0.38	134	135
28a	300	254	5.6	0.0	560	38.5	250	0.38	158	179

Table 2 Continued

Specimen	D [mm]	D' [mm]	ρl [%]	P [kN]	a [mm]	fc' [MPa]	fyh [MPa]	Ash/s [mm]	Vexp [kN]	Vnum [kN]
28b	300	254	5.6	0.0	560	38.5	250	0.38	175	179
37a	300	252	5.6	270.9	560	37.3	250	0.67	232	241
37b	300	252	5.6	0.0	560	37.3	250	0.67	218	201
38a	300	252	5.6	270.9	560	30.7	250	0.67	209	224
38b	300	252	5.6	0.0	560	30.7	250	0.67	206	187
39a	300	252	5.6	270.6	560	30.9	250	0.67	217	224
39b	300	252	5.6	0.0	560	30.9	250	0.67	197	188
40a	300	252	5.6	274.1	560	29.0	250	0.67	225	220
40b	300	252	5.6	0.0	560	29.0	250	0.67	183	183
43a	500	452	2.6	0.0	1100	32.1	250	0.72	313	378
43b	500	452	2.6	0.0	1100	32.1	250	0.72	366	378
44a	500	452	2.6	0.0	1100	28.0	250	0.72	301	359
44b	500	452	2.6	0.0	1100	28.0	250	0.72	329	359

can be used to evaluate θ for V_s in Eq. (15). In this sense, the proposed resistance mechanism for the analysis of the hoop contribution does not impose special restrictions. On the other hand, the deformation ε is intended as a constant "effective" value of the hoop strain localized in the neighborhood of a crack. Its real value should be measured experimentally or obtained indirectly from laboratory tests.

The proposed analytical model can be further developed to obtain more information about ε, i.e. a correlation between the hoop deformation and the crack width. In fact, it must be pointed out that, for sake of simplicity, a constant (localized in the neighborhood of a crack) value of the hoop strain ε is assumed, even if a more advanced model should consider its variability. A relevant consequence of this assumption is that the crack width $\overline{\mathrm{BB}'}$ is not constant along the column. On the contrary, it depends on the angle ψ (if the crack occurs in the lower part of the columns) or ω (if the crack occurs in the upper part of the column). If the crack is placed in the lower part of the column, then the following equation holds:

$$\frac{\overline{\mathrm{BB}'}}{2R} = (1+\varepsilon)\delta_\psi \sin(\psi + 2\delta_\psi) - \sin\delta_\psi \sin(\psi + \delta_\psi). \tag{17}$$

For a crack placed on the upper part of the column, a similar relation is obtained:

$$\frac{\overline{\mathrm{BB}'}}{2R} = (1+\varepsilon)\delta_\omega \sin(\omega + 2\delta_\omega) - \sin\delta_\omega \sin(\omega + \delta_\omega). \tag{18}$$

Therefore, the average value of the crack width can be determined as follows:

$$\left\langle \frac{\overline{\mathrm{BB}'}}{2R} \right\rangle = \frac{1}{(\pi - \omega_n)} \left\{ \int_0^{\pi/2-\omega_n} \left[(1+\varepsilon)\delta_\omega \sin(\omega + 2\delta_\omega) - \sin\delta_\omega \sin(\omega + \delta_\omega) \right] \mathrm{d}\omega \right.$$
$$\left. + \int_0^{\pi/2} \left[(1+\varepsilon)\delta_\psi \sin(\psi + 2\delta_\psi) - \sin\delta_\psi \sin(\psi + \delta_\psi) \right] \mathrm{d}\psi \right\}, \qquad (19)$$

where ω_n is the value of ω corresponding to the neutral axis position. Equation (19) provides further information about the hoop deformation ε. For instance, a numerical evaluation of the integral in Eq. (19) shows that $\left\langle \overline{\mathrm{BB}'} / (2R) \right\rangle$ is equal to 0.00156 for an effective localized strain ε equal to 4/100. This average value of the crack width seems to be fully acceptable and confirms that the concrete contribution is still present when the crack is open.

3. Comparison of predictions and experimental results

3.1 Database of experimental data

Numerical and experimental data are now compared. The numerically predicted shear capacity and the experimental one are denoted as V_{num} and V_{exp}, respectively. V_{num} is obtained as in Eq. (1), in which the concrete shear capacity and the reinforcement shear capacity are calculated as in Eq. (2) and Eq. (15), respectively. The considered database includes experimental data presented by Clarke and Birjandi (1993), McDaniel (1997) and Hamilton *et al*. (2002). Experimental data from (Clarke and Birjandi 1993) are listed in Table 2 (the symbol *D*’ denotes the diameter of the confined core).

3.2 Results and discussion

The exact neutral axis position for each specimen has been calculated in order to obtain the numerical shear strength value. In doing so, a parabola-rectangular diagram is assumed for modeling the stress-strain relationship in concrete whereas a linearly elastic-perfectly plastic stress-strain relationship is considered for modeling the reinforcement. Predicted shear strength values and experimental results from Clarke and Birjandi (1993) are listed in Table 2. The V_{num}/V_{exp} values obtained by means of the model proposed in this study are listed in Table 3, and they are compared with those in (Clarke and Birjandi 1993) and (Jensen and Hoang 2009). The adopted numerical value for ε in Table 2 and Table 3 is 4/100. The calculated mean value over the considered set of specimens is 1.01 (see Table 3, row “*Mean*”), which is appreciably better than the mean value obtained by Clarke and Birjandi (1993). It is also in excellent agreement with the mean value obtained by Jensen and Hoang (2009). The standard deviation value calculated using the presented model is 0.15 (see Table 3, row “*Std*”), which is close to that calculated by Clarke and Birjandi (1993), whereas it is 1.5 times the value obtained by Jensen and Hoang (2009).

Experimental data from (Clarke and Birjandi 1993), (McDaniel 1997) and (Hamilton *et al*. 2002),

Table 3 Comparison with two existing shear capacity models (Clarke and Birjandi 1993, Jensen and Hoang 2009)

Specimen	Clarke and Birjandi (1993) V_{exp}/V_{num}	Jensen and Hoang (2009) V_{exp}/V_{num}	This study V_{exp}/V_{num}
M1/2	1.25	0.95	1.02
M1/3	1.33	0.99	1.04
M1/4	1.10	0.83	0.86
7a	1.50	1.12	1.81
11a	1.58	1.09	1.15
11b	1.60	1.10	1.16
12a	1.37	0.90	0.98
12b	1.55	1.02	1.12
13a	1.63	1.03	1.09
13b	1.64	1.03	1.09
14a	1.57	0.96	1.04
14b	1.62	1.00	1.08
15a	1.35	1.00	1.02
15b	1.37	1.02	1.04
16a	1.48	1.01	1.04
16b	1.49	1.02	1.04
17a	1.43	1.10	1.11
17b	1.40	1.08	1.09
19a	1.21	0.88	0.92
19b	1.38	1.01	1.04
20a	1.35	0.91	0.95
20b	1.24	0.84	0.87
21a	1.32	0.91	0.98
21b	1.52	1.05	1.13
22a	1.35	0.84	0.91
22b	1.36	0.85	0.91
23a	1.28	0.93	0.94
23b	1.43	1.04	1.05
24a	1.21	0.81	0.82
24b	1.36	0.91	0.92
25a	1.13	0.79	0.83
25b	1.40	0.99	1.02
26a	1.09	0.71	0.74
26b	1.44	0.93	0.97
27a	1.31	1.04	1.07
27b	1.40	0.92	1.00
28a	1.36	0.82	0.88
28b	1.51	0.91	0.98
37a	1.50	1.09	0.96
37b	1.61	1.03	1.08
38a	1.42	1.06	0.93
38b	1.59	1.04	1.10
39a	1.47	1.10	0.97

Table 3 Continued

Specimen	Clarke and Birjandi (1993) Vexp/Vnum	Jensen and Hoang (2009) Vexp/Vnum	This study Vexp/Vnum
39b	1.52	1.00	1.05
40a	1.54	1.16	1.02
40b	1.43	0.95	1.00
43a	1.25	0.92	0.83
43b	1.46	1.08	0.97
44a	1.24	0.93	0.84
44b	1.36	1.01	0.92
Mean	*1.41*	*0.97*	*1.01*
Std	*0.14*	*0.10*	*0.15*

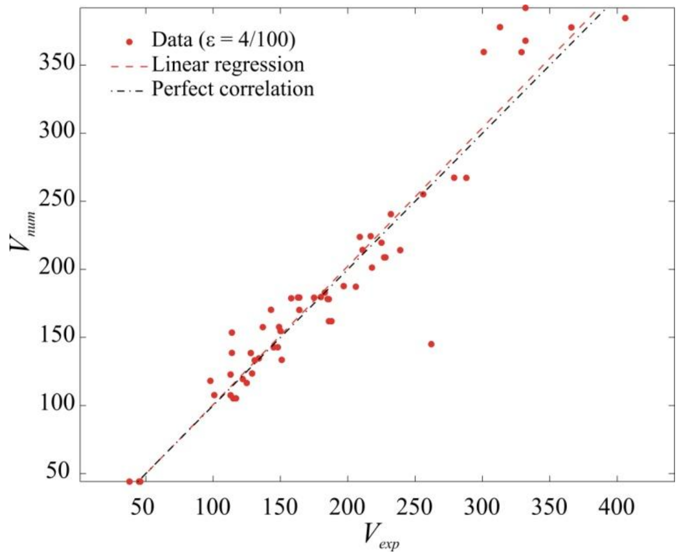

Fig. 3 Theoretical vs. experimental shear strength values (ε = 4/100)

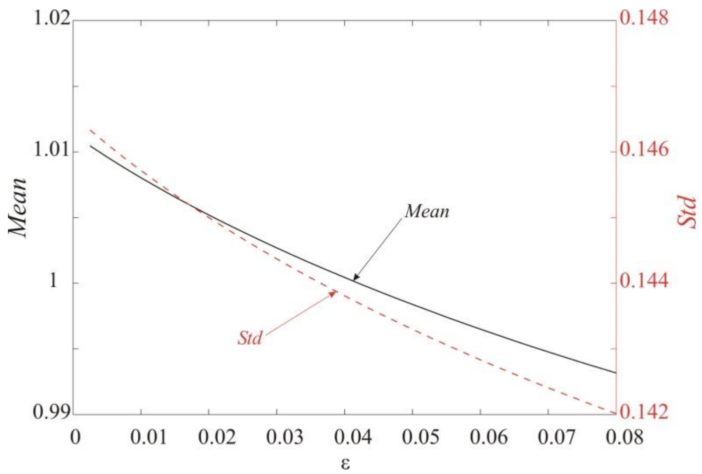

Fig. 4 Sensitivity analysis for ε.

together with the corresponding numerical predictions, are presented in Fig. 3. A sensitivity analysis for ε is also shown in Fig. 4. Based on this numerical analysis, it can be concluded that the proposed reinforcement shear capacity model appears physically consistent and numerically comparable to existing models. As a consequence, the proposed analytical model highlights an effective mechanism by which the hoops contribute to the total shear capacity in circular RC columns. It is expected, however, that a better approximation of the experimental data can be obtained by varying θ and ε appropriately.

4. Conclusions

This paper proposed a resistance mechanism, not yet considered in previous works, for the assessment of the hoop contribution to the total shear capacity in circular RC columns. In particular, it has been noted that, even for small crack widths, the slope of the hoops does not match the original one in the neighborhood of a crack. Moving from this physical observation, a simple analytical formulation for determining the reinforcement shear capacity was developed. The results obtained using the proposed model have been compared with experimental data, and a satisfactory agreement is found. It is worth highlighting that the proposed analytical model involves the assessment of the hoop strain localized in the neighborhood of a crack, but a different formulation of the considered resistance mechanism based on the crack width rather than the hoop strain can be explored.

References

Ang, B.G., Priestley, M.J.N. and Paulay, T. (1989), "Seismic shear strength of circular reinforced concrete columns", *ACI Struct. J.*, **86**(1), 45-59.

British Standards Institution (1990), *BS 5400 Steel, concrete and composite bridges: Part 4: Code of practice for design of concrete bridges*, London, UK.

Caglar, N. (2009), "Neural network based approach for determining the shear strength of circular reinforced concrete columns", *Constr. Build. Mat.*, **23**(10), 3225-3232.

Clarke, J.L. and Birjandi, F.K. (1993), "The behaviour of reinforced concrete circular sections in shear", *Struct. Eng.*, **71**(5), 73-81.

Hamilton, C.H., Pardoen, G.C. and Kazanjy, R.P. (2002), *Experimental Testing of Bridge Columns Subjected to Reversed-Cyclic and Pulse-Type Loading Histories*, Report 2001-03, Civil Engineering Technical Report Series, University of California, Irvine.

Jensen, U.G. and Hoang, L.C. (2009), "Shear strength prediction of circular RC members by the crack sliding model", *Mag. Conc. Res.*, **61**(9), 691-703.

Jensen, U.G. Hoang, L.C., Joergensen, H.B. and Fabrin, L.S. (2010), "Shear strength of heavily reinforced concrete members with circular cross section", *Eng. Struct.*, **32**(3), 617-626.

Kowalsky, M.J. and Priestley M.J.N. (2000), "Improved analytical model for shear strength of circular reinforced concrete columns in seismic regions", *ACI Struct. J.*, **97**(3), 388-396.

McDaniel, C. (1997), *Scale effects on the shear strength of circular reinforced concrete columns*, M.Sc. Thesis, University of California, San Diego.

Merta, I. (2007), "Shear strength model of reinforced concrete circular cross-section members", *Recent Developments in Structural Engineering, Mechanics and Computation*, A. Zingoni (Hrg.); Millpress Science Publishers, Rotterdam, The Netherlands.

Priestley, M.J.N., Seible, F. and Calvi, M. (1996), "Seismic design and retrofit of bridges", John Wiley &

Sons.
Priestly, M.J.N., Verma, R. and Xiao, Y. (1994), "Seismic shear strength of circular reinforced concrete columns", *J. Struct. Eng.-ASCE*, **120**(8), 2310-2329.
Sezen, H. (2008), "Shear deformation model for reinforced concrete columns", *Struct. Eng. Mech.*, **28**(1), 39-52.
Turmo, J., Ramos, G. and Aparicio, A.C. (2009), "Shear truss analogy for concrete members of solid and hollow circular cross section", *Eng. Struct.*, **31**(2), 455-465.
Wong, Y., Paulay, T. and Priestley, M.J.N. (1993), "Response of circular reinforced concrete columns to multi-directional seismic attack", *ACI Struct. J.*, **90**(2), 180-191.

CC